Ninth International Conference on Computational Fluid Dynamics (ICCFD9), Istanbul, Turkey, July 11-15, 2016 **ICCFD9**

A Numerical Investigation of Urine Flow Rate Effects on Stag Horn Stones Formation in a Kidney Ducts

[1]Sevda Aghaeizad, Seyed Esmail Razavi[1]& Farhad Sadegh Moghanlou[2]

[1]School of Mechanical Engineering, Tabriz University, Tabriz, Iran.

[2]School of Mechanical Engineering, Mohaghegh Ardabili University, Ardabil. Iran.

Corresponding author: sevda.aghz.1993@gmail.com

Abstract: The number of people suffering from kidney stones has increased. Stag horn stones are one of the dangerous and destructive kidney stone types. Urine flow rate plays a major rule in stag horn stones formation in kidney ducts. In this paper a 35-year-old man's kidney ducts is studied with computational fluid dynamics method. The paper presents the velocity field in a normal urine flow rate and shear rate in different urine flow rates by modeling 3D flow. The analysis performed in this study, can potentially lead to an improvement in the treatment of stag horn stones and enhance patient's living quality.

Keywords: Computational Fluid Dynamics, Laminar Flow, Kidney Stones, Navier-Stokes Equations.

1 Introduction

The urinary tract is the body's drainage system for removing urine, which is waste and harmful fluid. For normal urination, all body parts in the urinary system tract need to work together in the correct order.

The kidneys, as the main part of the urinary system, are bilaterally paired organs. Typically, each kidney weights 150 g in the males and 135 g in the females. They measures 10 to 12 cm vertically, 5 to 7 cm transversely and 3 cm in thickness [1]. According to the Figure 1, there are three major parts in the kidney, renal cortex, renal medulla and the renal pelvis. The outer layer is the renal cortex and the inner radially striated layer is the renal medulla [2].

The medulla is the inner tissue, which is surrounded by cortex and because of its shape is called medullary pyramid. This pyramid shaped structures end with minor calyces. As it shown in the Figure 2, the minor calyces join with three major calyces, which combining to form the renal pelvis.

The Renal pelvis is a tube that urine flows from the kidney to the urinary bladder, which connects the major calyces to the ureter [3].

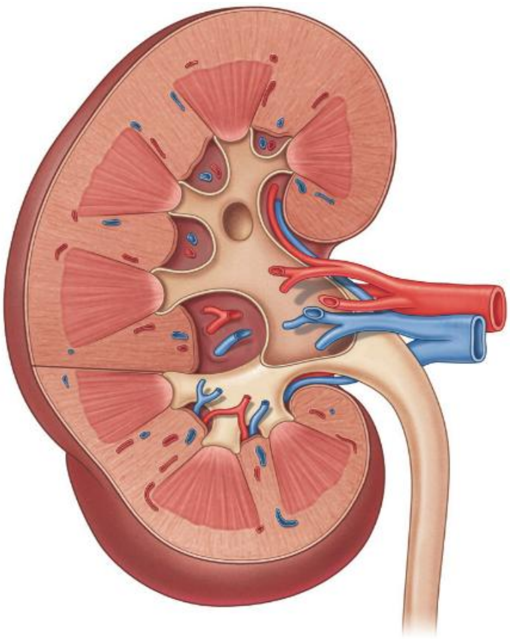

Figure1: Internal structure of the kidney [4].

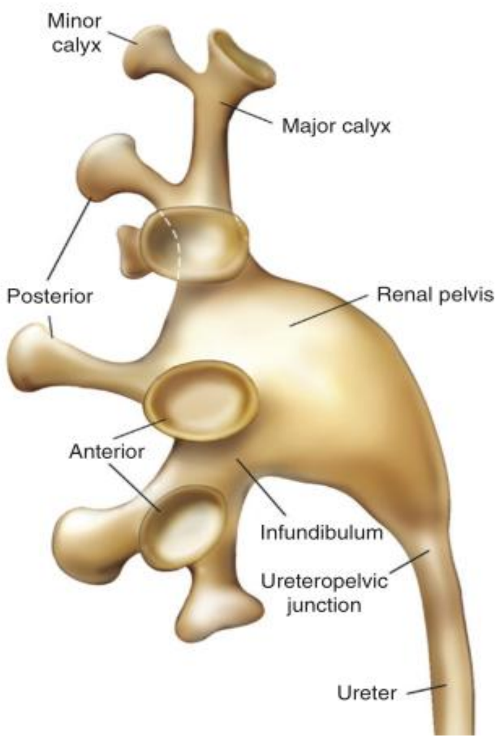

Figure2: Upper urinary tract collecting system [5].

The kidneys are composed of numerous urine collecting tubules that have the diameter of 20 mm and length of several millimeters [2]. They produce urine from water absorption; the absorbed water is taken to papillary ducts. There are 20 papillary ducts draining into each papilla, the renal papillae drain into the minor calyces. There are 5 to 14 minor calyces and three major calyces in each kidney [3]. The major calyces conduct the urine to renal pelvis.

Urinary tract stones begin to form in the kidney and may enlarge in the ureter or the bladder. Depending on where a stone is located, it may be called a kidney stone, ureteral stone, or bladder stone. Upper urinary tract stones that involve the renal pelvis and extend into at least 2 calyces are classified as stag horn calculi [3]. As shown in Figure 3, they fill the major part of the renal collecting system, mimicking the horns of a deer, which can lead extreme kidney damage.

An untreated stag horn stone is likely to destroy kidney and cause life-threatening sepsis. Patients associated with an untreated stag horn stone face an increased risk of death. Stone diseases affect men two or three times more often than women [6].

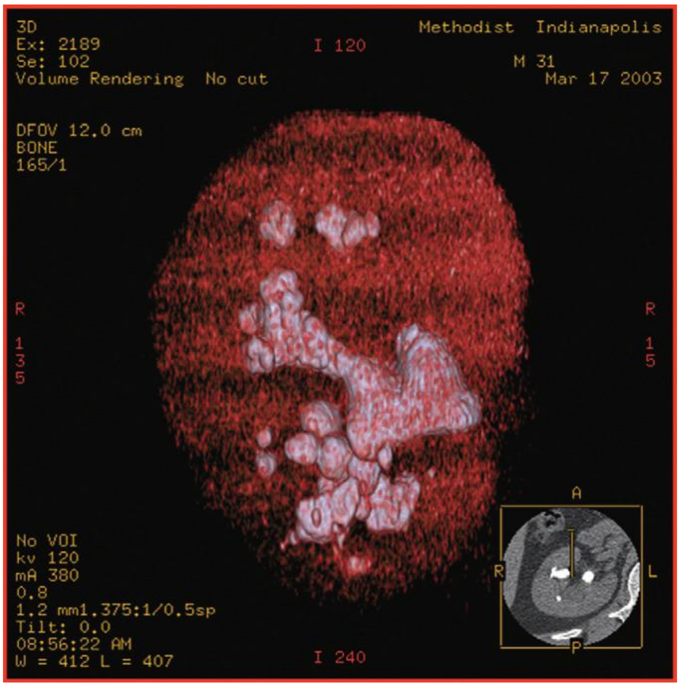

Figure 3: Three-dimensional CT-scan of stag horn stone [5].

Recent advances in CFD have made the realistic computational model of the urinary system possible. Wexler and. Marsh [7] formulated and solved a model of renal concentrating model.

Heimberg et al. [8] studied a new stone model in which artificial stones were constructed from the same chemical materials present in natural stones. The results indicate that the physical properties of artificial stones made of natural materials are comparable to renal calculi of the same chemical composition.

Kim et al. [9] numerically analyzed the urine flow in a stented ureter with no peristalsis, which was performed using a model based on the human anatomy. At their research, CFD simulation serves as tool to evaluate the effect of geometrical changes in stent design on urine flow and apply it to creating a new stent.

Najafi et al. [10] analyzed the peristaltic movement of ureter; furthermore, they investigated different types and shapes of stones in ureter and their effects on the urine flow and its pressure. It is concluded that in addition to the stone size, different stone shapes result in different pressures on the ureter wall. The result has led to develop a device based on measured injury forces.

Hoseini et al. [11] introduced a fluid-structure technique to study two contractions in a small tube mimicking human ureter. An increase in pressure and velocity is shown during the peristalsis around the ureter. They also modeled Viscoelastic behavior of the ureter.

Vahidi and Fatouraee [12] simulated a ureteral flow during peristalsis using intraluminal morphometric. The results showed that urine reflux to the kidney occur by the wave onset and the quantity of ureteropelvis reflux decrease by distally propagating the wave through the ureter.

There is lack of information about urine flow behavior through passages of kidney. In this study, the fluid flow in the upper urinary tract collecting system is simulated by means of computational fluid dynamics method. A three dimensional geometry based on real CT-Angiography pictures of the upper urinary tract collecting system of a 35-year-old man is investigate, which gives complete information about the flow field and introduce regions probable of stone formation. In addition, the effect of the three urine flow rate in the shear rate of specified localities are investigated.

2 Problem Statement

This paper employs a computational fluid dynamics (CFD) code to simulate the urine flow through the upper urinary tract collecting system of a kidney, which is the risky origin of stag horn stones formation. Three-dimensional CT-Angiography pictures of the upper urinary tract collecting system, including the minor calyces, major calyces, renal pelvis and a part of ureter, collected from a 35-year-old man who did not have any clinical history of urologic diseases, were used for the modeling. Figure 4 illustrates the samples of CT-Angiography photos. For realistic modeling, it has been used 16 photos from different angels of the kidney ducts.

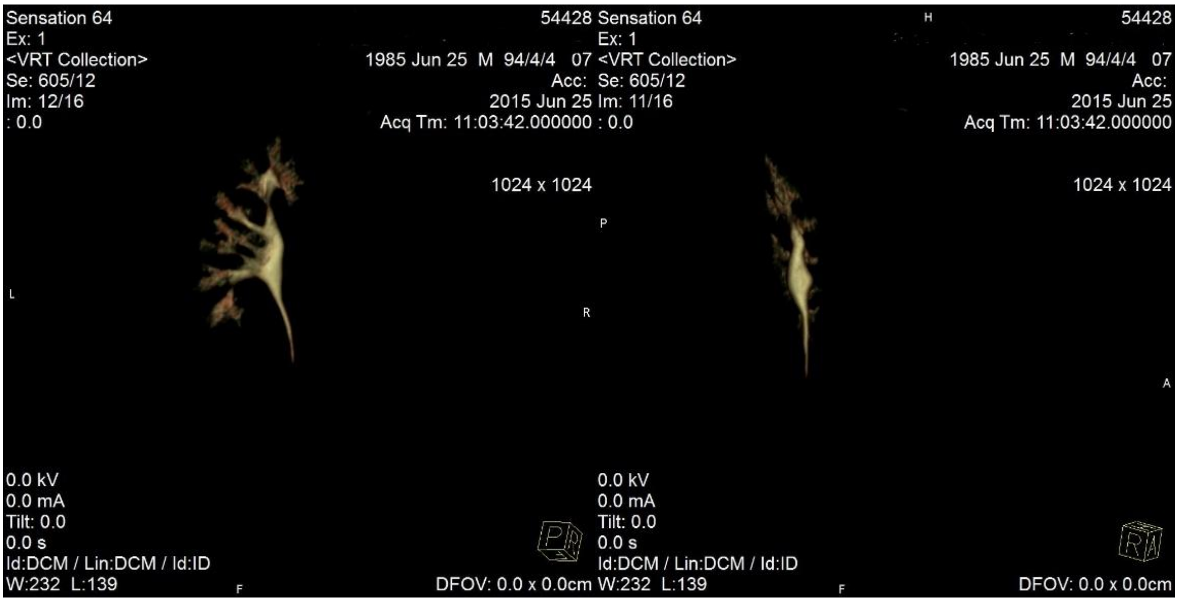

Figure 4: The samples of CT-Angiography photos.

Geometry of the numerical model extracted from Three-dimensional CT-Angiography pictures is presented in Figure 5, which has 11 inlets and one outlet. The whole length of upper urinary tract collecting system, is about 12 centimeters, and each inlet ranges from 2 to 5 millimeters in diameter. The outlet (ureter) is about 5 millimeters.

The urine flow is considered to be laminar, Newtonian, and incompressible. The urine density and dynamic viscosity at 37℃ are in the range of 1.0030-1.035 kg/m^3 and 0.635-0.797 mPa·s, respectively. The viscosity changes in the range of body temperature (35-40.5° C) is negligible [9].

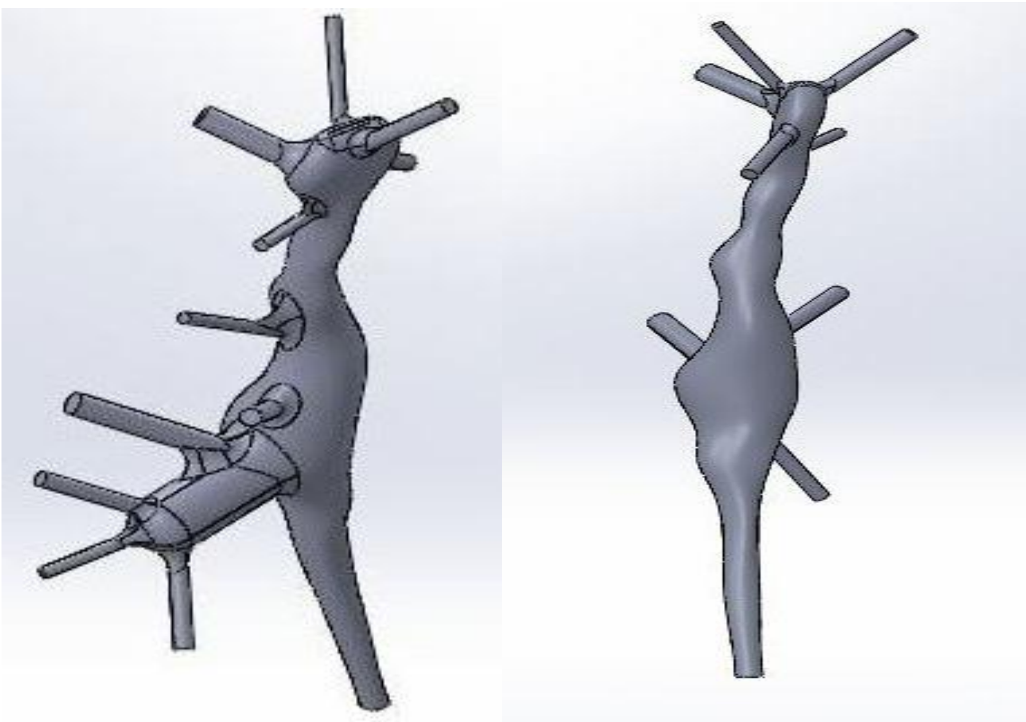

Figure5: Geometry of the model.

As shown in the Figure 6 the computational domain is meshed by hexahedral elements. Mesh independence obtained at 4×10^5 elements.

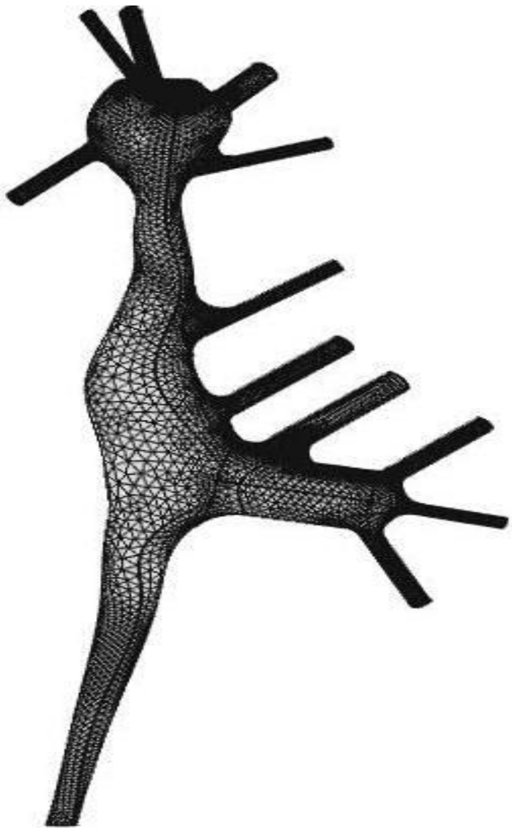

Figure 6: Solid domain mesh.

The walls of computational geometry is considered to be rigid so the governing equations are belong to fluid dynamics. The continuity and Navier-Stokes equation for incompressible fluid flow are respectively as:

$$\nabla.\mathrm{u} = 0$$

$$\rho \frac{\partial \mathrm{u}}{\partial t} + \rho(\mathrm{u}.\nabla)\mathrm{u} = \nabla.[-pI + \mu(\nabla \mathrm{u} + (\nabla \mathrm{u})^T)]$$

Where **ρ** and **μ** present urine density and dynamic viscosity respectively.

The computational domain includes 11 inlets where the mass flow through each of them is about 2.5E-5 kg/s for normal kidney function [13]. As inlet boundary condition, effects of the three urine flow rates (1E-5, 2.5E-5 and 5E-5) are investigated. The outlet has zero pressure condition.

Other sides of the domain is rigid wall and has no slip boundary condition.

3 Conclusion and Future Work

In the present work, three-dimensional simulation of upper urinary tract collecting system's urine flow is investigated numerically. Figures 7 and 8 show the velocity and shear rate distribution along the model in the normal urine flow rate respectively.

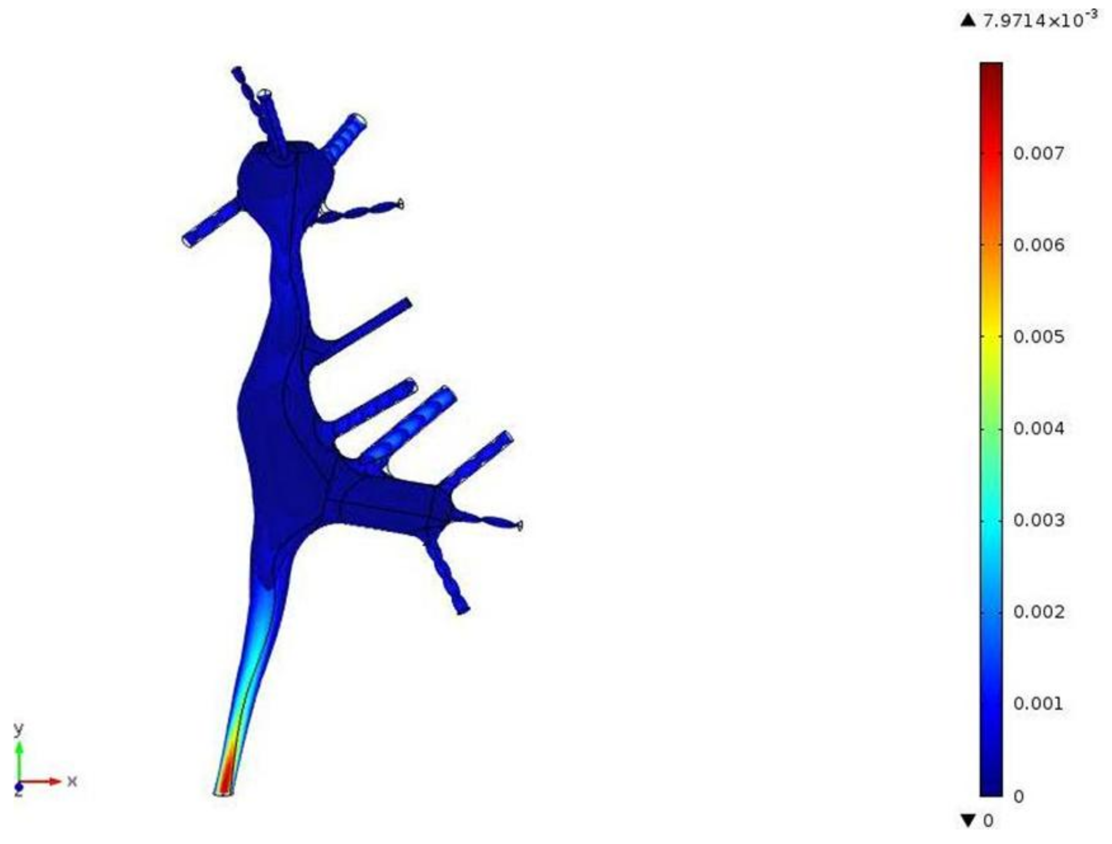

Figure7: The velocity field in a normal urine flow rate.

The velocity field shown in Figure 7 illustrates three different parts in upper urinary tract collecting system. The velocity field analysis of the urine flow shows a moderate value in minor calyces, low velocity in major and renal pelvis and high value in the ureter. As velocity reduces the risk of stone formation increases.

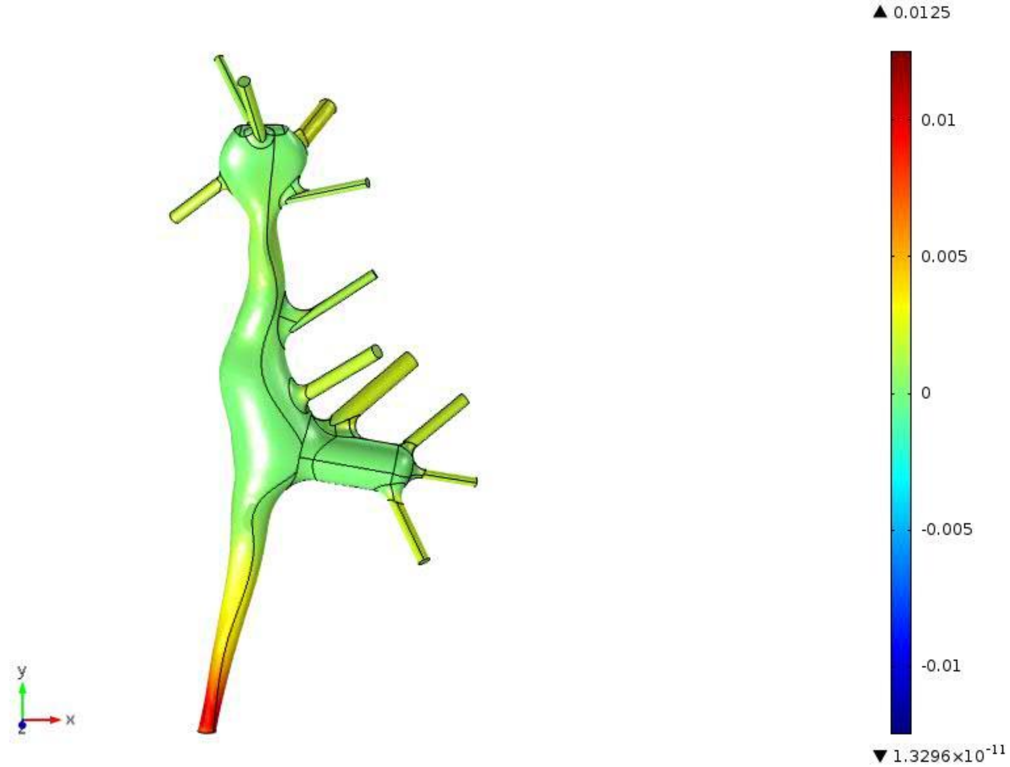

Figure 8: The shear rate field in a normal urine flow rate.

According to the shear rate shown in Figure 8 the renal pelvis and some sections of the major calyces have the minimum shear rate. The reduction in shear rate can lead to upset the delicate balance between the liquid and its solutes and will increase the stone formation risk [14]. Kidney stones usually comprised of a compound called calcium oxalate, are the result of an accumulation of dissolved minerals on the inner lining of the kidneys [15]. Almost zero shear rate area in the result, is seem to be the most likely region for accumulating of the minerals.

As the stone increases in size, the surface area available for additional mineral deposition is continually increased. Figure 9 shows the susceptible region more detailed.

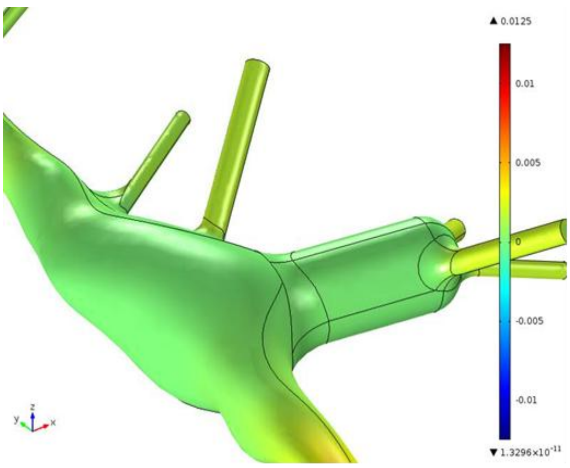

Figure 9: The shear rate field of susceptible region in a normal urine flow rate.

The susceptible region shown in Figure 9 is in accordance with the actual stag horn stones. Figure 10 shows an actual stag horn stone. The susceptible region introduced in this study is in accordance with the stag horn stones formed in kidneys.

Figure 10: A sample of a stag horn stone.

In the evaluation of three urine flow rates, this study aims to achieve a relation between the urine flow rate and shear rate values. Therefore, the shear rate value of individual localities in three urine flow rate as low, normal and high rates are studied and presented in the Table 1. Figure 11 shows the exact location of the elected localities.

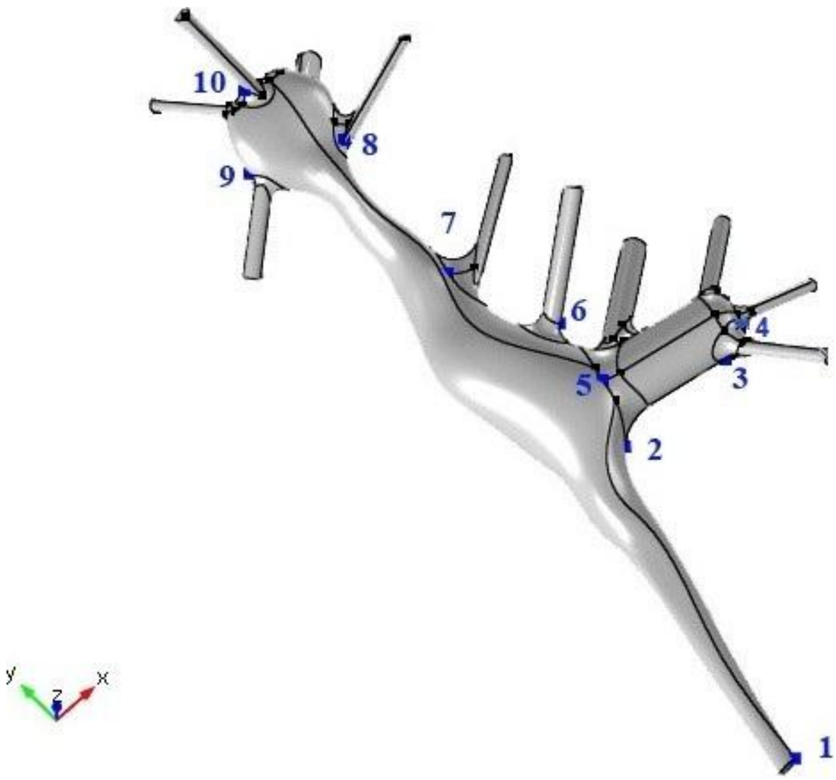

Figure 11: The exact location of the 10 localities.

Table1. The relation between flow rate and shear rate.

localities	**Low rate 1E-5 (kg/s)**	**Normal rate 2.5E-5 (kg/s)**	**High rate 5E-5 (kg/s)**
1	0.0045	0.0107	0.02083
2	1.35E-04	3.53E-04	7.56E-04
3	5.03E-05	1.23E-04	2.39E-04
4	7.09E-04	1.76E-03	3.49E-03
5	3.73E-05	9.49E-05	1.97E-04
6	6.66E-04	1.65E-03	0.00328
7	1.38E-04	3.47E-04	6.99E-04
8	1.77E-04	4.50E-04	9.19E-04
9	3.32E-05	7.55E-05	1.28E-04
10	6.31E-04	1.56E-03	0.00308

On analysis of the effect of urine flow rate on the shear rate in different localities, it is observed a significant relation of these two values, which increasing the flow rate will enhance the shear rate and decrease the risk of stone formation. Increasing the urine flow rate is performed with specific drugs. Diuretics, also called water pills, belong to a class of medications that are designed to increase the urine flow rate. They may be prescribed for kidney diseases and lowering the risk of stone formations [16].

In this paper, a numerical simulation of the upper urinary tract collecting system with a realistic geometry is analyzed. The analysis is performed to improve the understanding of the urine flow's behavior in kidney ducts. Furthermore, the susceptible region for stag horn stone formation is introduced and the effect of urine flow rate on stag horn stones formation studied. The outcome results of the three urine flow rates illustrated the shear rates role in stone forming. The numerical results may be helpful for experts in the field of experimental biomedicine to develop the treatments of kidney's stag horn stones.

References

[1] Anderson, J. K., J. N. Kabalin, and J. A. Cadeddu. "Surgical anatomy of the retroperitoneum, adrenals, kidneys, and ureters." Campbell-Walsh Urology 1 (2007): 34-37.

[2] “Internal Anatomy of the Kidneys.” Boundless Anatomy and Physiology. Boundless, 26 May. 2016. Retrieved 28 Jun. 2016.

[3] Gleeson MJ, Griffith DP. Infection Stones. Resnick MI, Pak CYC, eds. Urolithiasis: A Medical and Surgical Reference. Philadelphia, PA: Saunders; 1990. 134-36.

[4] Drake, Richard, A. Wayne Vogl, and Adam WM Mitchell. Gray's anatomy for students. Elsevier Health Sciences, 2014.

[5] Wolf, J. S. "Percutaneous approaches to the upper urinary tract collecting system." Campbell-Walsh Urology 10 (2012): 1324-56.

[6] Pearle, Margaret S., and Yair Lotan. "Urinary lithiasis: etiology, epidemiology, and pathogenesis." Campbell-walsh urology 2 (2007): 1363-92.

[7] Wexler, Anthony S., and Donald J. Marsh. "Numerical methods for three-dimensional models of the urine concentrating mechanism." Applied mathematics and computation 45.2 (1991): 219-240.

[8] Heimbach, D., et al. "Acoustic and mechanical properties of artificial stones in comparison to natural kidney stones." The Journal of urology 164.2 (2000): 537-544.

[9] Kim, Hyoung-Ho, et al. "Numerical analysis of the urine flow in a stented ureter with no peristalsis." Bio-Medical Materials and Engineering 26.s1 (2015): S215-S223.

[10] Najafi, Zahra. Development of new treatment modalities for kidney/ureter stones. Diss. The University of Akron, 2015.

[11] Hosseini, Ghazaleh, et al. "Computational simulation of urinary system." San Francisco, USA: Proc World Congress Eng Comput Sci. 2012.

[12] Vahidi, Bahman, and Nasser Fatouraee. "A biomechanical simulation of ureteral flow during peristalsis using intraluminal morphometric data." Journal of theoretical biology 298 (2012): 42-50.

[13] Hall, John E. Guyton and Hall textbook of medical physiology. Elsevier Health Sciences, 2015.

[14] Lingeman, James E., Brian R. Matlaga, and Andrew P. Evan. "Surgical management of upper urinary tract calculi." *Campbell-Walsh Urology* 2 (2007): 9.

[15] Creighton Medical Center, Mayo Clinic, Medical News Today archives, National Health Service.

[16] Diuretics. (2010, December 16). Mayo Clinic. Retrieved May 18, 2013.